Available online at www.sciencedirect.com
SCIENCE DIRECT
Colloids and Surfaces B: Biointerfaces 47 (2006) 165–175
COLLOIDS AND SURFACES B
www.elsevier.com/locate/colsurfb

Langmuir monolayer properties of the fluorinated-hydrogenated hybrid amphiphiles with dipalmitoylphosphatidylcholine (DPPC)

Kazuki Hoda [a], Hiromichi Nakahara [a], Shohei Nakamura [b], Shigemi Nagadome [c], Gohsuke Sugihara [c], Norio Yoshino [d,e], Osamu Shibata [a,*]

[a] *Division of Biointerfacial Science, Graduate School of Pharmaceutical Sciences, Kyushu University, 3-1-1 Maidashi, Higashi-ku, Fukuoka 812-8582, Japan*
[b] *College of Pharmaceutical Sciences, Daichi University, 22-1 Tamagawa-cho Minami-ku, Fukuoka 815-8511, Japan*
[c] *Department of Chemistry, Faculty of Science, Fukuoka University, 8-19-1 Nanakuma, Jyonan-ku, Fukuoka 814-0180, Japan*
[d] *Department of Industrial Chemistry, Faculty of Engineering, Tokyo University of Science, 1-3 Kagurazaka, Shinjuku-ku, Tokyo 162-8601, Japan*
[e] *Institute of Colloid and Interface science, Tokyo University of Science, 1-3 Kagurazaka, Shinjuku-ku, Tokyo 162-8601, Japan*

Received 15 October 2005; received in revised form 3 December 2005; accepted 11 December 2005
Available online 19 January 2006

Abstract

Surface pressure–area (π–A), surface potential–area (ΔV–A), and dipole moment–area ($\mu_{\perp}$–A) isotherms were obtained for the Langmuir monolayer of two fluorinated-hydrogenated hybrid amphiphiles (sodium phenyl 1-[(4-perfluorohexyl)-phenyl]-1-hexylphosphate (F6PH5PPhNa) and (sodium phenyl 1-[(4-perfluorooctyl)-phenyl]-1-hexylphosphate (F8PH5PPhNa)), DPPC and their two-component systems at the air/water interface. Monolayers spread on 0.02 M Tris buffer solution (pH 7.4) with 0.13 M NaCl at 298.2 K were investigated by the Wilhelmy method, ionizing electrode method and fluorescence microscopy. Moreover, the miscibility of two components was examined by plotting the variation of the molecular area and the surface potential as a function of the molar fraction for the fluorinated-hydrogenated hybrid amphiphiles on the basis of the additivity rule. The miscibility of the monlayers was also examined by construction of two-dimensional phase diagrams. Furthermore, assuming the regular surface mixture, the Joos equation for analysis of the collapse pressure of two-component monolayers allowed calculation of the interaction parameter (ξ) and the interaction energy ($-\Delta\varepsilon$) between the fluorinated-hydrogenated hybrid amphiphiles and DPPC. The observations by a fluorescence microscopy also supported our interpretation as for the miscibility in the monolayer state. Comparing the monolayer behavior between the two binary systems, no remarkable difference was found among various aspects. Among the two combinations, the mole fraction dependence in monlayer properties was commonly classified into two ranges: $0 \leq X \leq 0.3$ and $0.3 < X \leq 1$. Dependence of the chain length of fluorinated part was reflected for the molecular packing and surface potential.

Keywords: Fluorinated compound; Fluorinated-hydrogenated hybrid amphiphiphile; Dipalmitoylphosphatidylcholine (DPPC); Langmuir monolayer; Surface pressure; Surface potential; Fluorescence microscopy

1. Introduction

Fluorinated surfactants are particularly valuable when extreme surface activity, hydrophobicity, lipophobicity, resistance to high temperatures, aggressive chemical or biological environments, and detergent activity are needed [1,2]. Wide scale of newly well-defined and modular fluorinated surfactants were recently synthesized, allowing the preparation and stabilization of various colloidal systems with potential biomedical applications. For example, a neat fluorocarbon, fluorocarbon-in-water emulsion, and reverse water (or hydrocarbon)-in-fluorocarbon emulsion are being evaluated for in vivo oxygen delivery, liquid ventilation, diagnosis and drug delivery [3–5].

In order to develop performance of surfactants recently, the so-called "hybrid" type surfactants with a hydrocarbon and a fluorocarbon chain in an identical molecule have been synthesized

* Corresponding author. Tel.: +81 92 642 6669; fax: +81 92 642 6669.
E-mail address: shibata@phar.kyushu-u.ac.jp (O. Shibata).
URL: http://210.233.60.66/∼kaimen/.

0927-7765/$ – see front matter © 2005 Elsevier B.V. All rights reserved.
doi:10.1016/j.colsurfb.2005.12.006

[6]. Though fluorocarbon chain length of these materials is not so long enough in general, they have various unique properties such as ability to reduce the surface tension of water, simultaneous emulsification of hydrocarbon oil/fluorocarbon oil/water [7], formation of small micelles with unusually long lifetime [8], and very high viscosity of the surfactant solution at body heat [9–13]. Their applications are highly expected in the chemical, mechanical and other industrial aspects. For example, fluorocarbon-hydrocarbon hybrid surfactants having a phenyl phosphate group do adsorb on teeth to give hydrophobicity as well as lipophobicity to the surface and their micelles solubilizing dental drugs can penetrate into periodontal pockets in order to cure periodontal disease [6]. We have previously investigated a mixed system made of a phospholipid (dipalmitoylphosphatidylcholine, DPPC) and hydrogenated or perfluorocarboxylic acids from our interest in mechanism of anesthesia, because most of local anesthetics are halogenated organic compounds. Hence, the conclusion that the interaction of DPPC with fluorocarbon fatty acids is stronger than that with hydrocarbon ones was reached [14–16]. Some other papers on two-component system of partially fluorinated carboxylic acid and phospholipid Langmuir monolayer have already appeared [17–20]. Nevertheless, little is known about the factors determining the phase behavior of mixtures of these hybrid surfactants with a hydrocarbon chain and a fluorocarbon chain in an identical molecule in their monolayer states.

Due to the importance or usefulness of hybrid amphiphiles in advanced clinical trials [1,2,21–23], it is necessary to know the way how these hybrid materials do interact with their given environments. In this respect, studies on two-component monolayers of the hybrid amphiphiles and phospholipids are assumed to work as a basic model system reflecting the two dimensional interaction modes. Phospholipids have attracted a great attention because they are one of the most abundant ingredients in cell membranes [24]. Among the many different phospholipids, DPPC has been employed for binary monolayer studies in many cases [25–30]. They reported that fluorocarboxylic acids and DPPC were partially miscible in the binary monolayers. Intermolecular interaction was rather strong, suggesting that attractive forces between head groups contribute more to miscibility than the hydrophobic interactions [14,15].

We in this study have focused on characterizing the Langmuir monolayer behavior of two hybrid amphiphiles (F6PH5PPhNa and F8PH5PPhNa), DPPC and their two-component systems at the air/water interface. The surface pressure (π)–, surface potential (ΔV)–, and dipole moment ($\mu_\perp$)–A isotherms were obtained for the respective pure systems and their two-component systems. Phase diagrams plotting the collapse pressure (π^c) against the molar fraction of F6PH5PPhNa (or F8PH5PPhNa) were constructed, and were examined for the respective binary systems in comparison with the simulated curves of ideal mixing based on the Joos equation [31]. Finally, the monolayers were examined by fluorescence microscopy [32,33]. It is noted that the present study on the two fluorinated-hydrogenated hybrid amphiphiles/DPPC binary systems is further being extended from the view point of a partial molecular area (PMA), an apparent partial molecular surface potential (APSP), a surface excess Gibbs energy and its thermodynamic analysis based on the regular solution theory, the compressibility of the formed monolayer film and the hysteresis phenomenon in π–A curves accompanied by compression and expansion; the results and discussion will be reported in a separate paper.

2. Experimental

Sodium phenyl 1-[(4-perfluorohexyl)-phenyl]-1-hexylphosphate (which is denoted as F6PH5PPhNa or F6) and Sodium phenyl 1-[(4-perfluorooctyl)-phenyl]-1-hexylphosphate (which is denoted as F8PH5PPhNa or F8) were synthesized and purified as reported previously [6]. Their chemical structures are demonstrated in Fig. 1. Dipalmitoylphosphatidylcholine (L-α-1-palmitoyl-2-hydroxy-sn-glycero-3-phosphocholine: DPPC, purity >99%) was purchased from Avanti Polar Lipids Inc. (Birmingham, AL, USA) and used without further purification. Stock solutions of the respective samples (1 mM) were prepared in a mixed solvent of *n*-hexane/ethanol mixture (9/1 in v/v) which were purchased from nacalai tesque, and 50 μL of the respective mixed solution was spread at the air/aqueous solution interface. The spreading solvent was allowed to evaporate for 15 min prior to compression. The buffer solution used as the substrate was prepared using thrice distilled water (surface tension, 72.7 mN m^{-1} at 293.2 K; resistivity, 18 MΩ cm) with a 0.02 M Tris (hydroxymethyl) aminomethane (Tris) buffering agent and with 0.13 M NaCl, and its pH was adjusted to be 7.4 with adequate addition of acetic acid (HAc). Sodium chloride (nacalai tesque) was roasted at 1023 K for 24 h to remove any surface active organic impurity.

2.1. Surface pressure–area (π–A) isotherms

The surface pressure (π) was measured using an automated homemade Wilhelmy film balance. The surface pressure balance (Mettler Toledo, AG245) has a resolution of 0.01 mN m^{-1}. The pressure-measuring system was equipped with a filter paper (Whatman 541, periphery 4 cm). A trough made from a 720 cm^2 Teflon-coated brass was used. The π–A isothems were recorded at 298.2 ± 0.05 K. The monolayers were compressed at a speed of 0.13 nm^2 molecules^{-1} min^{-1}. The standard deviations for area and surface pressure measurements were ∼0.01 nm^2 and ∼0.1 mN m^{-1}, respectively.

2.2. Surface potential (ΔV) measurements as a function of area (A)

Surface potential was recorded upon compression of the monolayer spread on 0.02 M Tris buffer solution with 0.13 M NaCl at 298.2 K. It was monitored using an ionizing ^{241}Am electrode placed 1–2 mm above the interface, while a reference electrode was dipped into the subphase. The standard deviation for the surface potential measurements was ∼±2.5 mV. The other conditions were the same as described in previous papers [34]. The ΔV–A data were transfered to surface dipole moment ($\mu_\perp$) by computer as reported in the literature [34].

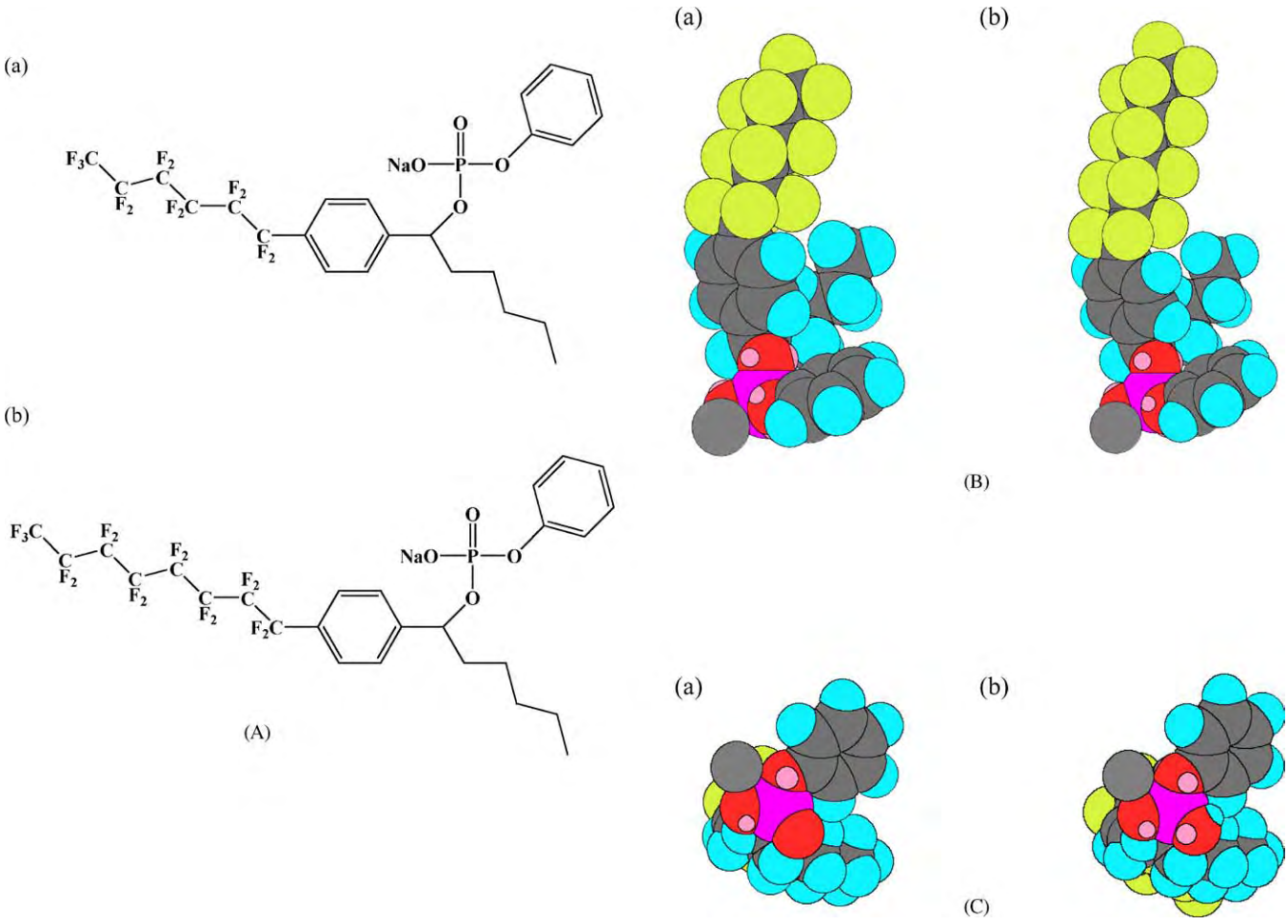

Fig. 1. F6PH5PPhNa (a) and F8PH5PPhNa (b) molecules in skelton chemical structure (A), broad side view (B), and bird's-eye view from the beneath (C).

2.3. Fluorescence microscopy

Fluorescence images were observed using an automated homemade Wilhelmy film balance equipped with a fluorescence microscope (BM-1000, U.S.I. System, Japan). It is possible to record simultaneously the surface pressure (π)–area (A) and the surface potential (ΔV)–A isothems along with the monolayer images in order to correlate these properties of the same monolayer. A 300 W lamp (XL 300, Pneum) was used for fluorescence excitation. A 546 nm band path filter (Mitutoyo) was used for excitation and a 590 nm cut-off filter (Olympus) for emission. The monolayer images were taken using a 20× long-distance objective lens (Mitutoyo f = 200/focal length 20 mm). A xanthylium 3,6-bis(diethylamino)-9-(2-octadecyloxycarbonyl) phenyl chloride (R18, Molecular Probes) was used as an insoluble fluorescent probe. It has its absorbance and emission band maxima at 556 and 578 nm, respectively. The solution containing 1 mol% of the fluorescent probe against insoluble materials was used in the fluorescence microscopy experiments. Fluorescence images were recorded, with a CCD camera (757 JAI ICCD camera, Denmark) connected to the microscope, directly into computer memory through an online image processor (VAIO PCV-R53, Sony: video capture soft). The entire optical set-up was placed on an active vibration isolation unit (Model-AY-1812, Visolator, Japan). The operation of the present microscopy was similar to the previous reports [35,36].

3. Results and discussion

3.1. Stability of the F6PH5PPhNa and F8PH5PPhNa monolayers

To check the monolayer's stability, the relaxation time of the surface pressure after compression up to 35 mN m^{-1} was measured for F6PH5PPhNa, F8PH5PPhNa and DPPC. A 0.02 M Tris buffer solution with 0.13 M NaCl was chosen as the subphase in order to mimic a biomembrane-like environment. Fig. 2 shows that the surface pressure of DPPC decreased during the first 30 min and then plateaued at ca. 33 mN m^{-1}. This value is in good agreement with literature value [32]. On the other hand, even though small decreasing in the surface pressure was observed for the F6PH5PPhNa and F8PH5PPhNa monolayers even after 1 h, their aqueous solubilities are so low that both species can hardly exist in bulk solution (substrate phase). They are enough stable to form the insoluble monolayer at the air/water interface.

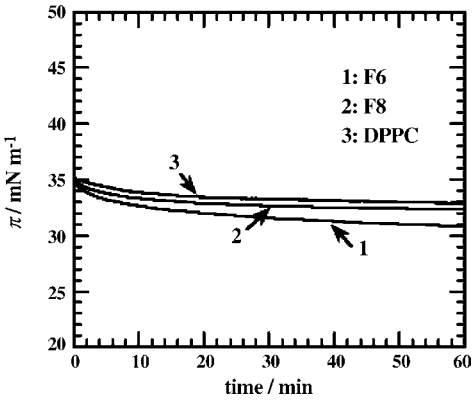

Fig. 2. Time dependence of the surface pressure (π). Langmuir monolayers were compressed up to 35 m Nm^{-1} on 0.02 M Tris buffer solution with 0.13 M NaCl at 298.2 K; the π–t measurements were then started. 1: F6PH5PPhNa; 2: F8PH5PPhNa, and 3: DPPC.

3.2. Isotherms of surface pressure (π), surface potential (ΔV), and dipole moment ($\mu_\perp$) versus area per molecule (A)

The π–A, ΔV–A and $\mu_\perp$–A isotherms of monolayers formed by the respective single systems of F6PH5PPhNa, F8PH5PPhNa, and DPPC on 0.02 M Tris buffer solution (pH 7.4) with 0.13 M NaCl at 298.2 K are shown in Fig. 3. The π–A isothems demonstrate that extrapolated surface areas of the F6PH5PPhNa and F8PH5PPhNa are almost the same but much larger than that of DPPC. The high compressibility of the hybrid surfactants over whole surface pressure range as well as the absence of discontinuity in their π–A isotherms shows that both single systems do spread over the surface as a typical disorder monolayer. The monolayer of F6PH5PPhNa was confirmed to be stable up to 43.5 mN m^{-1}, which is confirmed by the collapse pressure for F6PH5PPhNa and by its ΔV measurement. The extrapolated area (limiting area A_0) in the closed packing state was estimated to be 0.89 nm^2. Originally, the cross sectional area of an optimally packed, all *trans*, hydrocarbon chain is about 0.20 nm^2 and that of a fluorocarbon chain is about 0.30 nm^2. Then the hydrophobic portions of the hybrid double-chain molecules may be expected to occupy an area of $A = 0.20 + 0.30 = 0.50$ nm^2. But the observed value is much larger than 0.50 nm^2. The large extrapolated area (nm^2) reflects the bulkiness of the fluorinated-hydrogenated hybrid amphiphiles' hydrophobic tail moiety coming from their bond angle due to the existence of two benzene rings, whereas conformation of their two hydrophobic chains is judged to be *para* type (see Fig. 1).

The collapse pressure and the extrapolated area for F8PH5PPhNa are ~44.5 mN m^{-1} and 0.87 nm^2, respectively. Compared with the π–A isotherm of pure F6PH5PPhNa (43.5 mN m^{-1} and 0.89 nm^2) shown in Fig. 3, no remarkable difference can be seen in π–A isotherm between them. This indicates that the extension of fluorinated chain length has no influence upon the monolayer property and its two-dimensional area. Fig. 1B and C, respectively, include the broad side view and bird's-eye view from beneath which shows the cross section corresponding to the extrapolated surface area.

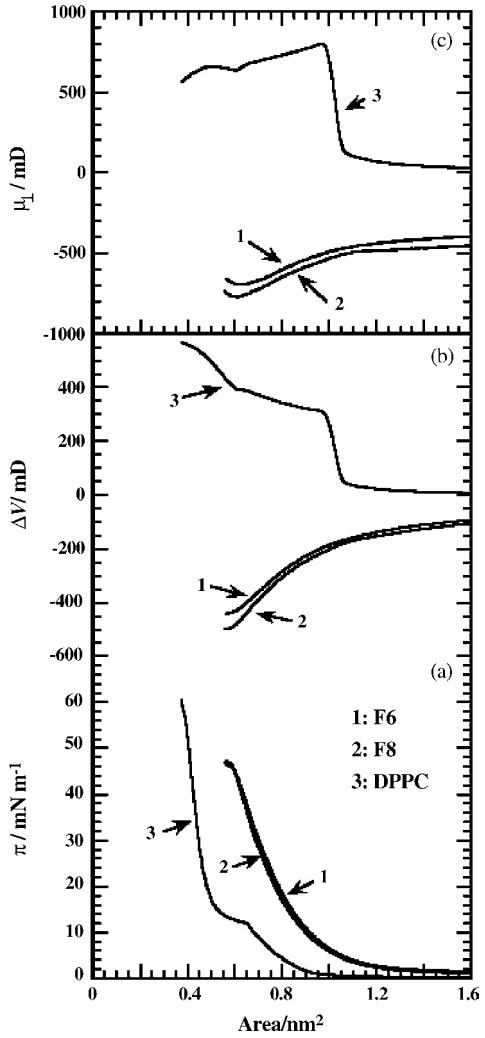

Fig. 3. Surface pressure (π)–area (A) isotherms (a), surface potential (ΔV)–A isotherms (b), and surface dipole moment ($\mu_\perp$)–A isotherms (c) of F6PH5PPhNa (F6): 1, F8PH5PPhNa (F8): 2 and DPPC: 3 on 0.02 M Tris buffer solution with 0.13 M NaCl at 298.2 K.

On the other hand, the DPPC isotherm presented the characteristic first-order phase transition from the disordered liquid-expanded (LE) phase to the ordered liquid-condensed (LC) phase. The transition pressure (π^{eq}) at 298.2 K was 11.8 mN m^{-1}, above which the surface pressure went up accompanying the conformational change. The collapse pressure and the extrapolated area of DPPC were found to be 55 mN m^{-1} and 0.49 nm^2, respectively. These values are very close to those previously reported [32,37–39] except for minor distinctions caused by difference in subpahse composition.

Fig. 3(b) and (c) frames show the variations of ΔV and $\mu_\perp$ as a function of molecular surface area for F6PH5PPhNa, F8PH5PPhNa, and DPPC monolayers, respectively. The surface potential (ΔV) is a measure of the electrostatic field gradient perpendicular to the horizontal surface and thus varies considerably with the molecular surface density. The behavior of ΔV–A isotherms corresponds to the change of the molecular orientation upon compression as shown in Fig. 3. In the surface potential values (ΔV), both F6PH5PPhNa and F8PH5PPhNa always

keep the negative. The ΔV values at the closest packed state reach around −440 mV for F6PH5PPhNa and around −497 mV for F8PH5PPhNa. The negative values attribute to the fluorocarbon chain and the greater value of F8PH5PPhNa than that of F6PH5PPhNa results from the closer packing of the former. In contrast, the DPPC monolayer has the positive ΔV value of 558 mV at high surface pressure. Markedly abrupt change in the ΔV–A curve for DPPC indicates great change in the orientation, corresponding to a change from gas state to LE, while both hybrid surfactants exhibit a gradual change of conformation of floating molecules on the surface with compression.

The vertical component of surface dipole moment ($\mu_\perp$) was calculated from the Helmholtz equation using the measured values of ΔV,

$$\mu_\perp = \Delta V \varepsilon_0 \varepsilon A \quad (1)$$

where ε_0 is the permittivity of a vacuum (which is assumed to be unity) and ε is the mean permittivity of the monolayer, A is the area occupied by a molecule [40]. The ΔV or $\mu_\perp$ values involve the resultant change of the dipole moments carried by the polar head, the hydrophobic groups (the hydrocarbon chain group, the fluorocarbon chain group, and phenyl group), and the subphase. The respective changing modes of $\mu_\perp$ with compression are shown in Fig. 3c, indicating a big difference between DPPC and hybrid surfactants, as similar to that of ΔV–A behavior.

3.3. Miscibility of two-component systems

First of all, for the two combinations of two-component monolayer systems composed of F6PH5PPhNa, F8PH5PPhNa, and DPPC, it is indispensable to clarify the effect of molecular structure, the interaction between two components, and the miscibility in the monolayer state. For the above purposes, the π–A, ΔV–A and $\mu_\perp$–A isotherms were obtained at various compositions at 298.2 K on a 0.02 M Tris buffer solution with 0.13 M NaCl for F6PH5PPhNa/DPPC and F8PH5PPhNa/DPPC systems.

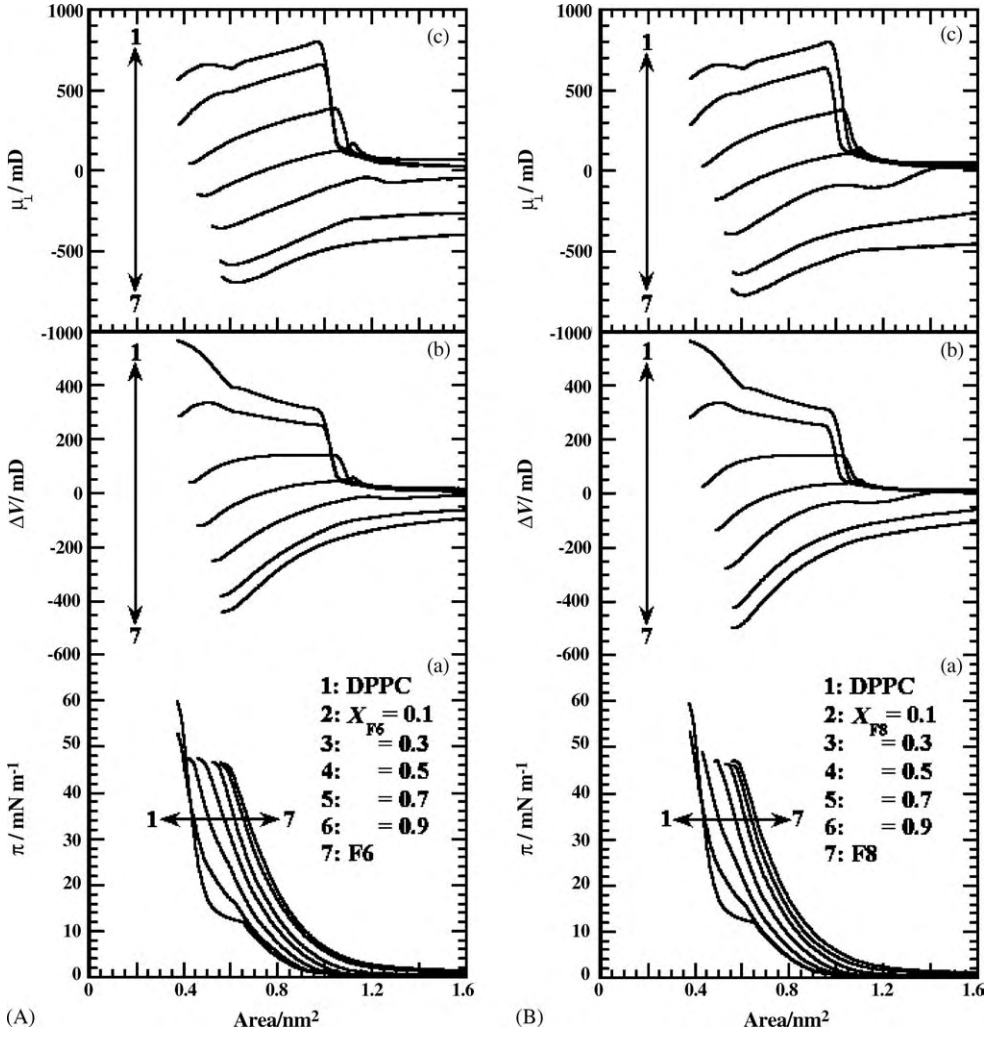

Fig. 4. (A) Surface pressure (π)–area (A) isotherms (a), surface potential (ΔV)–A isotherms (b), and surface dipole moment ($\mu_\perp$)–A isotherms (c) of F6PH5PPhNa/DPPC two-component monolayers as a function of F6PH5PPhNa molar fraction (X_{F6}) on 0.02 M Tris buffer solution with 0.13 M NaCl at 298.2 K. (B) Surface pressure (π)–area (A) isotherms (a), surface potential (ΔV)–A isotherms (b), and surface dipole moment ($\mu_\perp$)–A isotherms (c) of F8PH5PPhNa/DPPC two-component monolayers as a function of F6PH5PPhNa molar fraction (X_{F8}) on 0.02 M Tris buffer solution with 0.13 M NaCl at 298.2 K.

3.3.1. F6PH5PPhNa and F8PH5PPhNa/DPPC two-component systems

Fig. 4A and B exhibits the π–A isotherms for two-component monolayers of F6PH5PPhNa/DPPC and F8PH5PPhNa/DPPC systems at various mole fractions, respectively. All the isotherms of the binary systems sit in the order of the increase in the mole fraction between those of both single systems. The transition from disorder to order was observable up to X_{F6} (or X_{F8}) = 0.3. The change and disappearance of the transition pressure with increasing surface pressure suggests that F6PH5PPhNa and F8PH5PPhNa have an ability to make DPPC miscible in the monolayers, as mentioned in the later section of two-dimensional phase diagram. This observation is the first evidence that these two components are well miscible with DPPC in the monolayer. As it is difficult to ascertain the presence of the transition pressure at the mole fractions >0.3 on the π–A isotherms, we have investigated these two systems by fluorescence microscopy (later section).

The interaction between F6PH5PPhNa or F8PH5PPhNa and DPPC molecules was investigated by examining whether the variation of the mean molecular areas (A_m) as a function of X_{F6} (or X_{F8}) can satisfy the additivity rule or not [41]. Comparison between the experimental A_m values and those of ideal mixing (dashed straight line) is shown in Fig. 5a and b at four surface pressures (5, 15, 25, and 35 mN m^{-1}). For π = 5 mN m^{-1}, both F6PH5PPhNa/DPPC and F8PH5PPhNa/DPPC systems show a small negative deviation from the additivity rule, indicating a weak attractive interaction between them. This may result from the fact that at such low surface pressures the interactions between them are mainly governed by the attractions between the polar heads. In contrast, for π = 15, and 25 mN m^{-1}, positive deviations are observed, reflecting the coexistence region of LE and LC states of DPPC. But at π = 35 mN m^{-1}, the variation almost follows the additivity rule. This indicates that these two components are almost ideally mixed in the monolayer state; the repulsion between the hydrocarbon chain and fluorocarbon chain is compensated by the attractive interaction between the head groups of these two components, as has been observed for DPPC/perfluorocarboxylic acid two-component monolayers [14]. Looking at the curves at 35 mN m^{-1} for both two-component systems in more detail, in the range below X_{F6} or X_{F8} = 0.3 the A_m values deviate negatively, while the curves above 0.3 deviate positively. This suggests that the two-component monolayer state may be divided at least into two parts above and below the mole fraction of 0.3. In addition, there is no remarkable difference between the two combinations. A binary system can show apparently an ideal behavior, when the two components form an ideally mixed monolayer or the two components can not mixed completely but can form the so-called patched film. Even in the latter case, the additivity should show a linear relation as indicated by a broken line. So, such a direct observation as fluorescence microscopy may be useful, to determine whether both components do form really well mixed films or form patched films.

Turning our attention to the influence of X_{F6} (or X_{F8}) on the ΔV–A and $\mu_\perp$–A isotherms shown in Fig. 4A and B, both the surface potential (ΔV) and the surface dipole moment ($\mu_\perp$) clearly indicate that all the curves of the two-component systems

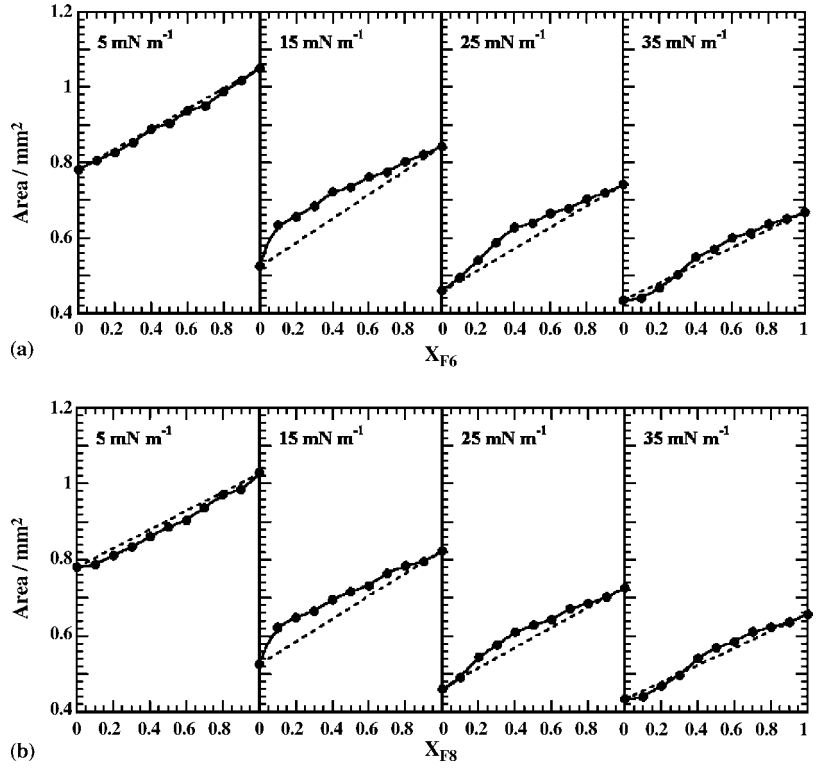

Fig. 5. Mean molecular area (A_m) of F6PH5PPhNa/DPPC (a) and F8PH5PPhNa/DPPC (b) two-component systems as a function of the composition of F6PH5PPhNa (F6) or F8PH5PPhNa (F8) at four different pressures. The dashed lines represent the additivity rule, and the solid circles do the experimental values.

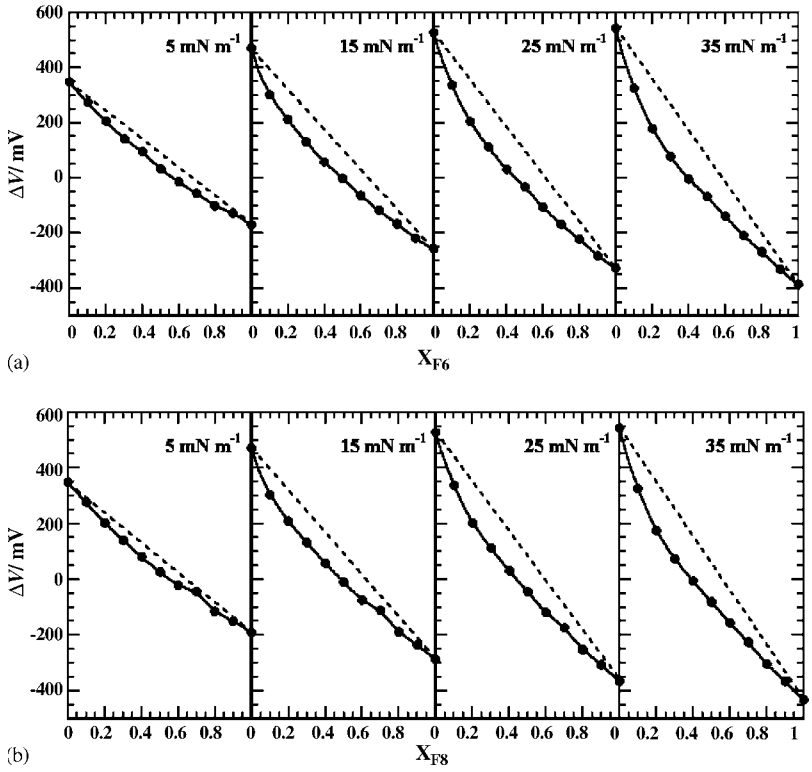

Fig. 6. Surface potential (ΔV) of F6PH5PPhNa/DPPC (a) and F8PH5PPhNa/DPPC (b) two-component systems as a function of the composition of F6PH5PPhNa (X_{F6}) or F8PH5PPhNa (X_{F8}) at four different pressures. The dashed lines represent the additivity rule, and the solid circles do the experimental values.

locate between those of the respective pure components and that they successively change with the mole fraction. Analysis of the surface potential (ΔV) of the two-component monolayers in terms of the additivity rule is presented in Fig. 6a and b. For both these two-component systems, comparison of the experimental data values with calculated ones (dashed line) clearly indicates the negative deviations at all surface pressures. The profiles of deviation are almost similar between F6PH5PPhNa/DPPC and F8PH5PPhNa/DPPC systems, which suggests that the effect of extending fluorocarbon chain length for their conformation is not very remarkable because of the same tilt angle between their double chains.

From all the curves given in Figs. 3 and 4, the fundamental data values such as transition pressure (π^{eq}), collapse pressure (π^{c}), and absolute surface potential (ΔV) at the closed packing state in addition to limiting area (A_0) were determined and tabulated in Table 1 as a function of X_{F6} (or X_{F8}).

3.4. Two-dimensional phase diagrams

From the π–A isotherms for the two-component systems of F6PH5PPhNa/DPPC and F8PH5PPhNa/DPPC, their two-dimensional phase diagrams were constructed using the data of the transition pressure (π^{eq}) and the collapse pressure (π^{c}) changes at various molar fractions of F6PH5PPhNa or F8PH5PPhNa. Resultant phase diagrams at 298.2 K are shown in Fig. 7A and B, respectively.

Firstly, in F6PH5PPhNa/DPPC system, the transition pressures from disorder (gaseous or liquid-expanded) to order

Table 1
Fundamental data of monolayer properties for F6PH5PPhNa/DPPC and F8PH5PPhNa/DPPC two-component systems; extrapolated molecular surface area (A_0), transition pressure (π^{eq}), collapse pressure (π^{c}), and surface potential (ΔV)

Mole fraction, X	A_0 (nm^2)	π^{eq} ($mN\,m^{-1}$)	π^{c} ($mN\,m^{-1}$)	ΔV (mV)
F6PH5PPhNa/DPPC system				
0.0	0.49	11.8	54.9	550
0.1	0.55	15.6	52.0	290
0.2	0.60	22.9	49.2	140
0.3	0.67	26.9	46.5	38
0.4	0.75		45.7	−53
0.5	0.78		45.2	−120
0.6	0.80		44.9	−190
0.7	0.81		44.1	−250
0.8	0.84		44.1	−310
0.9	0.85		44.0	−380
1.0	0.89		43.5	−440
F8PH5PPhNa/DPPC system				
0.0	0.49	11.8	54.9	550
0.1	0.55	15.8	52.2	280
0.2	0.60	22.6	49.4	120
0.3	0.66	27.7	46.5	23
0.4	0.74		46.1	−68
0.5	0.76		45.6	−140
0.6	0.77		45.2	−200
0.7	0.79		44.9	−280
0.8	0.81		44.8	−350
0.9	0.83		44.7	−420
1.0	0.87		44.5	−500

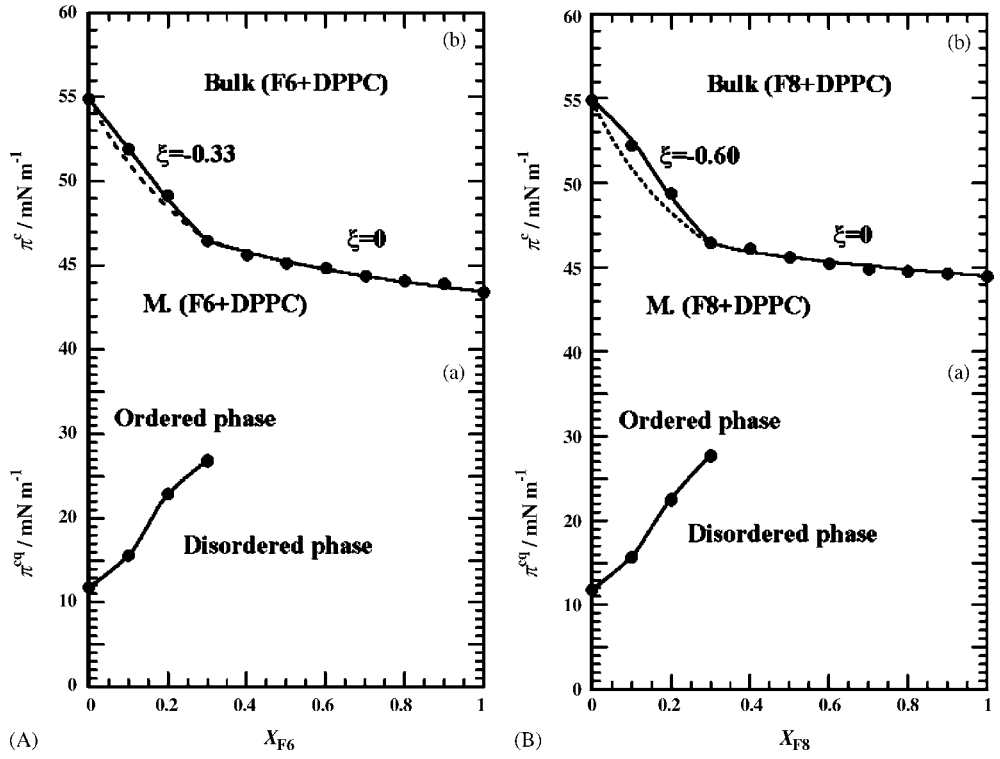

Fig. 7. (A) The phase diagram of F6PH5PPhNa/DPPC system on 0.02 M Tris buffer solution with 0.13 M NaCl at 298.2 K. (a) The transition pressure (π^{eq}) and (b) the collapse pressure (π^c) plotted against mole fraction of F6PH5PPhNa (X_{F6}). The dashed line was calculated by Eq. (2) in the case of $\xi = 0$. (B) The phase diagram of F8PH5PPhNa/DPPC system on 0.02 M Tris buffer solution with 0.13 M NaCl at 298.2 K. (a) The transition pressure (π^{eq}) and (b) the collapse pressure (π^c) plotted against mole fraction of F8PH5PPhNa (X_{F8}). The dashed line was calculated by Eq. (2) in the case of $\xi = 0$.

(liquid-condensed) phase are plotted against mole fraction of F6PH5PPhNa in Fig. 7A-(a). In this system at $X_{F6} = 0$–0.3, π–A isotherm displays a phase transition pressure (π^{eq}) that changes almost linearly with X_{F6}. Judging from the change of the transition pressure, two components are miscible each other at mole fractions, which is the first evidence of the miscibility of the two components within the monolayer films as described above. This can be explained by the fact that film-forming molecules become more dense by compression, accompanying more depression in surface tension by the film-forming molecules themselves. Then the resultant surface pressure was raised. The rise in the transition pressure with mole fraction of F6PH5PPhNa means that the transition of DPPC takes place when the film-forming molecules become denser with the mole fraction. These phenomena resemble the elevation of boiling point and the depression of freezing point in the mixed solution.

Assuming that the surface mixtures behave as a surface regular solution with a hexagonal lattice, the coexistence phase boundary between the ordered monolayer phase and the bulk phase can be theoretically simulated by the following Joos equation, and the interaction parameter (ξ) can be calculated from this deviation [31] too:

where x_1^s and x_2^s denote the mole fraction in a given binary mixed monolayer composed of components 1 and 2, respectively, and π_1^c and π_2^c are the corresponding collapse pressures of components 1 and 2. π_m^c ($m = 1$, 2) is the collapse pressure of the monolayer at given composition of x_1^s and x_2^s. ω_1 and ω_2 are the corresponding limiting molecular surface area at the collapse points. γ^1 and γ^2 are the surface activity coefficients at the collapse point, ξ the interaction parameter, and kT is the product of the Boltmann constant and the Kelvin temperature. The solid curve is made coincident with the expemental values by adjusting ξ.

In these figures, M. indicates a two-component monolayer formed by F6PH5PPhNa and DPPC species, while bulk denotes a solid phase of F6PH5PPhNa and DPPC ("bulk phase" may be called "solid phase"). The collapse pressure π^c determined at each mole fraction is indicated by filled circles, where the dotted line shows the case where the interaction parameter (ξ) is zero for an ideal mixing.

From the diagram, the new finding is that the monolayer state of F6PH5PPhNa/DPPC two-component system can be divided into two regions; that is $\xi = -0.33$ at the range of $X_{F6} = 0$–0.3 and $\xi = 0$ at $X_{F6} = 0.3$–1. The negative interaction parameter means that there is mutual interaction between two components in the

$$1 = x_1^s \gamma^1 \, exp\left\{\frac{(\pi_m^c - \pi_1^c)\omega_1}{kT}\right\} \exp\left\{\xi (x_2^s)^2\right\} + x_2^s \gamma^2 \exp\left\{\frac{(\pi_m^c - \pi_2^c)\omega_2}{kT}\right\} \exp\left\{\xi (x_1^s)^2\right\} \quad (2)$$

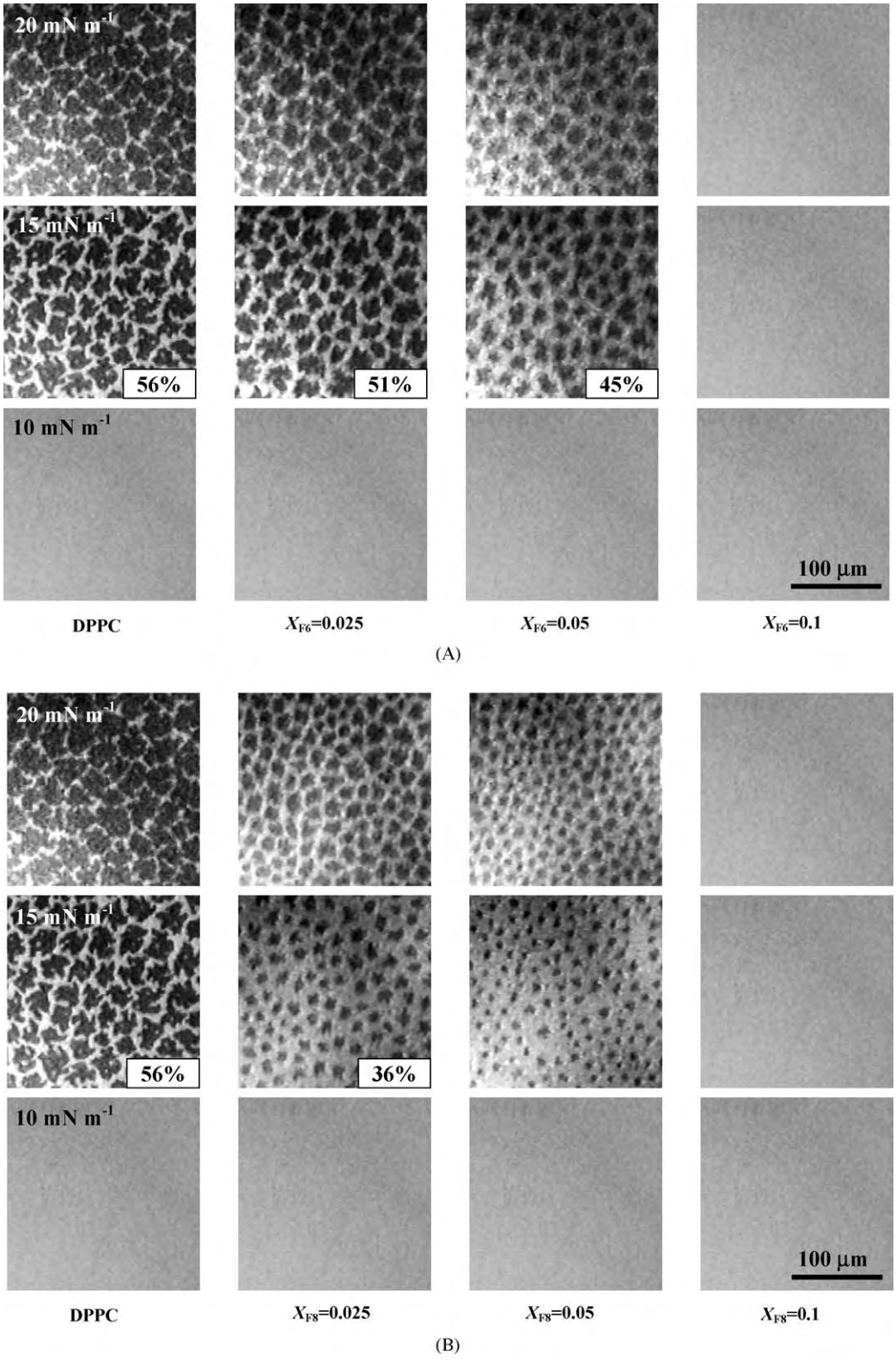

Fig. 8. (A) Fluorescence micrographs of F6PH5PPhNa/DPPC two-component monolayer at various mole fractions (X_{F6} = 0.025, 0.05, and 0.1) observed on 0.02 M Tris buffer solution with 0.13 M NaCl at 298.2 K. The monolayers contain 1 mol% fluorescent probe. The number in these images indicates the surface pressure and the order domain percentage in the micrograph. Scale bar represents 100 μm. (B) Fluorescence micrographs of F8PH5PPhNa/DPPC two-component monolayer at various mole fractions (X_{F8} = 0.025, 0.05, and 0.1) observed on 0.02 M Tris buffer solution with 0.13 M NaCl at 298.2 K. The monolayers contain 1 mol% fluorescent probe. The number in these images indicates the surface pressure and the order domain percentage in the micrograph. Scale bar represents 100 μm.

two-component monolayer that is stronger than the mean of the interactions between pure component molecules themselves. The interaction energy $-\Delta\varepsilon$ can be calculated by the following equation:

$$-\Delta\varepsilon = \frac{-\xi RT}{6} \quad (3)$$

And their interaction energies were calculated to be $-\Delta\varepsilon = 136\,\mathrm{J\,mol^{-1}}$ for a pair of F6PH5PPhNa and DPPC molecules in the range of $X_{F6} = 0$–0.3. As the result, F6PH5PPhNa and DPPC are completely miscible in the condense state as well as in the expanded state, and this behavior is classified into the positive azeotropic type.

Secondly, F8PH5PPhNa/DPPC system demonstrates that the monolayer behavior may also be divided into two parts at the mole fraction of $X_{F8} = 0.3$, similar to F6PH5PPhNa/DPPC system. Their interaction parameter and interaction energies were calculated to be $\xi = -0.60$ for the mixture in the range of $X_{F8} = 0$–0.3,($\xi = 0$ in $X_{F8} = 0.3$–1) and $-\Delta\varepsilon = 248\,\mathrm{J\,mol^{-1}}$, respectively. Thus, these two components in both combinations are regarded as complete mixing.

3.5. Fluorescence microscopy of monolayers formed by F6PH5PPhNa and F8PH5PPhNa/DPPC two-component systems

In order to interpret the phase behavior on the π–A isotherms, we investigated the morphological observation by fluorescence microscopy, which provides a direct picture of the monolayers. If a fluorescent dye probe is incorporated into the monolayer, its distribution can be determined by fluorescence microscopy. The contrast is due to difference in dye solubility between disorder (or LE) and order phases (or LC). Thus, we took fluorescence micrographs (FMs) of pure F6PH5PPhNa/DPPC and F8PH5PPhNa/DPPC two-component monolayers spread at 298.2 K on 0.02 M Tris buffer solution with 0.13 M NaCl as are shown in Fig. 8A and B at various surface pressures. Image analysis was performed using NIH image. The percentage in FM images indicates parts of order (or LC) domain.

Essentially, two phases of bright and dark contrast were observed for pure DPPC, which correspond to the LE matrix and LC domains, respectively [42–45]. It is known that the proportion of dark LC phase increases at the expense of the bright LE phase with surface pressure increasing. The DPPC monolayer on 0.02 M Tris buffer solution with 0.13 M NaCl develops LC domains in a qualitatively similar fashion as previously reported [46]. Angular, grain-like domains first appeared near the kink at $\sim$11.8 mN m^{-1}. They grew upon further compression to form distorted star-shaped domains with a blurred periphery that progressively formed a network. Above $\sim$21 mN m^{-1}, the images start to loose their crispness and the visual impression is of a progressive blurring of the domain boundaries. This blurring may be caused by the dissolution of the dye into the dye-depleted regions of the monolayer after the phase transition has been completed, i.e., when both the dye-enriched and the dye-depleted regions have become the same phase. Above 40 mN m^{-1}, it is likely that some of the probe molecules were inserted in the dark phase areas and the intensity of the probe in the bright (fluid) domains was observed to decrease of intensity, suggesting that self-quenching has occurred because of probe molecules coming in close contact with one another. The percentage is ratio of LC domain in each image to the total area.

Monolayers of pure F6PH5PPhNa and F8PH5PPhNa used in this study did not form the LC domains in the monolayer. As the result, FM shows the disorder image. The bright patterns in the FM image are the evidence of such disorder domains being independent of surface pressure.

The mole fraction dependence of the transition pressure is observed on the FM images of these two-component systems of F6PH5PPhNa/DPPC and F8PH5PPhNa/DPPC in Fig. 8A and B, respectively. At low surface pressures ($\pi < \pi^{eq}$), the two-component monolayer for F6PH5PPhNa/DPPC system uniformly fluoresced, showing apparently homogeneous disorder phase without order phase of dark domains. As increasing the surface pressure, order domains appeared from at $X_{F6} = 0.025$ to 0.05. In each case, the disorder/order coexistence region is observed, and the transition pressure (π^{eq}) is higher than that of pure DPPC. This suggests that the observed dark domains in these figures would represent a condensed DPPC-enriched phase. But we cannot capture the order domains above the mole fraction of $X_{F6} = 0.1$, although the transition pressure (π^{eq}) was observed up to $X_{F6} = 0.3$. With increasing surface pressure, the conformation change of the polar head groups in the two-component monolayer took place to facilitate the formation of the small order domains of DPPC. In this system, the small order domains were distributed homogeneously and observed to undergo the Brownian motion in the monolayer. At higher surface pressures, the growth of circular order domains persists in F6PH5PPhNa/DPPC two-component monolayer. As a result, this binary system was found to form not patched film but well mixed monolayer completely miscible each other.

In the FM image of F8PH5PPhNa/DPPC system (Fig. 8B), the similar behavior might be also observed for the F6PH5PPhNa/DPPC system. The difference between these two binary systems is that F8PH5PPhNa can more disperse the order domains of the DPPC than F6PH5PPhNa. This is supported by the percentage of order domain in each image as well as domain size.

4. Conclusions

Synthesized hybrid type surfactants with a hydrocarbon chain and a fluorocarbon chain in one molecule (F6PH5PPhNa and F8PH5PPhNa) can be spread as a stable monolayer on 0.02 M Tris buffer solution with 0.13 M NaCl at 298.2 K together with phospholipid (DPPC). The monolayer properties of F6PH5PPhNa, F8PH5PPhNa and DPPC, and both two-component systems of the two hybrids with DPPC, F6PH5PPhNa/DPPC and F8PH5PPhNa/DPPC were investigated at different compositions. The miscibility was supported by the changes of the transition pressure and the collapse pressure in the monolayer state over the surface pressures. The π–A, ΔV–A isotherms of F6PH5PPhNa/DPPC and F8PH5PPhNa/DPPC mixtures showed that the two

components were miscible in the monolayer state over the whole range of X_{F6} (or X_{F8}) and of surface pressures investigated. The two-dimensional phase diagram and the Joos equation allowed calculation of the interaction parameter (ξ) and interaction energy ($-\Delta\varepsilon$) for F6PH5PPhNa/DPPC and F8PH5PPhNa/DPPC systems. All these systems were classified as "positive azeotroic type". In these systems, π–A isotherm displays a phase transition pressure (π^{eq}) from $X = 0$ to 0.3 that changes almost linearly with X_{F6} (or X_{F8}). The observations using fluorescence microscopy also supported the miscibility in the monolayer state. The new finding that the present two binary monolayers can be divided at least into two parts above and below mole fraction of 0.3, which enables us to expect a developing perspective in regard to study on amphiphile mixtures.

Acknowledgments

This work (O. S.) was partially supported by Grant-in-aid for Scientific Research 17310075 from Japan Society for Promotion of Science and by Grant 17650139 from the Ministry of Education, Science and Culture, which are greatly appreciated.

The authors are grateful to Ms. Y. Morikawa for her contribution to the present study through the preliminary experiments and analysis from which important as well as useful information could be derived. This work was supported in part by funds from the Central Research Institute of Fukuoka University and from the advanced Material Institute of Fukuoka University.

References

[1] (a) M.P. Krafft, J.G. Riess, Biochimie 80 (1998) 489;
(b) J.G. Riess, Tetrahedron 58 (2002) 4113.
[2] (a) E. Kissa, Fluorinated Surfactants – Synthesis, Properties Applications, Surfactant Science Series vol. 50, Marcel Dekker, New York, 1994;
(b) E. Kissa, Fluorinated Surfactant and Repellents, Surfactant Science Series vol. 97, 2nd ed., Marcel Dekker, New York, 2001.
[3] J.G. Riess, M.P. Krafft, Biomaterials 19 (1998) 1529.
[4] M.P. Krafft, A. Chittofrati, J. Riess, Curr. Opin. Colloid Interf. Sci. 8 (2003) 251–258.
[5] J. Riess, Curr. Opin. Colloid Interf. Sci. 8 (2003) 259–266.
[6] H. Miyazawa, H. Yokokura, Y. Ohkubo, Y. Kondo, N. Yoshino, J. Fluorine Chem. 125 (2004) 1485.
[7] N. Yoshino, K. Hamano, Y. Omiya, Y. Kondo, A. Ito, M. Abe, Langmuir 11 (1995) 466.
[8] Y. Kondo, H. Miyazawa, H. Sakai, M. Abe, N. Yoshino, J. Am. Chem. Soc. 124 (2002) 6516.
[9] M. Abe, K. Tobita, H. Sakai, Y. Kondo, N. Yoshino, Y. Kasahara, H. Matsuzawa, M. Iwahashi, N. Momozawa, K. Nishiyama, Langmuir 13 (1997) 2932.
[10] K. Tobita, H. Sakai, Y. Kondo, N. Yoshino, M. Iwahashi, N. Momozawa, M. Abe, Langmuir 13 (1997) 5054.
[11] K. Tobita, H. Sakai, Y. Kondo, N. Yoshino, K. Kamogawa, N. Momozawa, M. Abe, Langmuir 14 (1998) 4753.
[12] M. Abe, K. Tobita, H. Sakai, K. Kamogawa, N. Momozawa, Y. Kondo, N. Yoshino, Colloids Surf. A: Physicochem. Eng. Aspects 167 (2000) 47.
[13] D. Danino, D. Weihs, R. Zana, G. Orädd, G. Lindblom, M. Abe, Y. Talmon, J. Colloid Interf. Sci. 259 (2003) 382.
[14] S. Yamamoto, O. Shibata, S. Lee, G. Sugihara, Prog. Anesth. Mech. 3 (Special Issue) (1995) 25.
[15] O. Shibata, S. Yamamoto, S. Lee, G. Sugihara, J. Colloid Interf. Sci. 184 (1996) 201.
[16] H. Nakahara, S. Nakamura, H. Kawasaki, O. Shibata, Colloid Surf. B 41 (2005) 283.
[17] H.-J. Lehmler, M. Jay, P.M. Bummer, Langmuir 16 (2000) 10161.
[18] H.-J. Lehmler, M.O. Oyewumi, M. Jay, P.M. Bummer, J. Fluorine Chem. 107 (2001) 141.
[19] H.-J. Lehmler, P.M. Bummer, J. Colloid Interf. Sci. 249 (2002) 381.
[20] M. Arora, P.M. Bummer, H.-J. Lehmler, Langmuir 19 (2003) 8843.
[21] M.P. Krafft, J.P. Rolland, P. Vierling, J.G. Riess, New J. Chem. 14 (1990) 869.
[22] M.P. Krafft, P. Vierling, J.G. Riess, Eur. J. Med. Chem. 26 (1991) 545.
[23] J.G. Riess, Chem. Rev. 101 (2001) 2797.
[24] L. Ter-Minassian-Saraga, J. Colloid Interf. Sci. 70 (1979) 245.
[25] K. Gong, S.H. Feng, Colloids Surf. A 207 (2002) 113.
[26] P. Mattijus, J.P. Slottle, Chem. Phys. Lipids 81 (1996) 69.
[27] P. Mattijus, R. Bittman, C. Vilchèze, J.P. Slottle, Biochim. Biophys. Acta 1240 (1995) 237.
[28] P. Dynarowicz-Latka, R. Seoane, J. Minones Jr., M. Velo, J. Minunes, Colloids Surf. B 27 (2002) 249.
[29] T.-H. Chou, C.-H. Chang, Colloids Surf. B 17 (2000) 71.
[30] M. Kodama, O. Shibata, S. Nakamura, S. Lee, G. Sugihara, Colloids Surf. B 33 (2004) 211.
[31] P. Joos, R.A. Demel, Biochim. Biophys. Acta 183 (1969) 447.
[32] T. Hiranita, S. Nakamura, M. Kawachi, H.M. Courrier, T.F. Vandamme, M.P. Krafft, O. Shibata, J. Colloid Interf. Sci. 265 (2003) 83.
[33] H. Nakahara, S. Nakamura, H. Kawasaki, O. Shibata, Colloids Surf. B 41 (2005) 285.
[34] (a) O. Shibata, Y. Moroi, M. Saito, R. Matuura, Langmuir 8 (1992) 1806;
(b) O. Shibata, Y. Moroi, M. Saito, R. Matuura, Thin Solid Films 242 (1994) 273;
(c) O. Shibata, H. Miyoshi, S. Nagadome, G. Sugihara, H. Igimi, J. Colloid Interf. Sci. 146 (1991) 594;
(d) H. Miyoshi, S. Nagadome, G. Sugihara, H. Kagimoto, Y. Ikawa, H. Igimi, O. Shibata, J. Colloid Interf. Sci. 149 (1992) 216;
(e) O. Shibata, Y. Moroi, M. Saito, R. Matuura, Thin Solid Films 327 (1998) 123;
(f) O. Shibata, M.P. Krafft, Langmuir 16 (2000) 10281.
[35] H. Nakahara, S. Nakamura, K. Nakamura, M. Inagaki, M. Aso, R. Higuchi, O. Shibata, Colloids Surf. B 42 (2005) 157.
[36] H. Nakahara, S. Nakamura, K. Nakamura, M. Inagaki, M. Aso, R. Higuchi, O. Shibata, Colloids Surf. B 42 (2005) 175.
[37] H. Morgan, D.M. Taylor, O.N. Oliveira Jr., Biochim. Biophys. Acta 1062 (1991) 149.
[38] V.L. Shapovalov, Thin Solid Films 327–329 (1998) 599.
[39] D. Honig, D. Möbius, Thin Solid Films 210–211 (1992) 64.
[40] J.H. Schulman, A.H. Hughes, Proc. R. Soc. (Lond.) A138 (1932) 430.
[41] (a) J. Marsden, J.H. Schulman, Trans. Faraday Soc. 34 (1938) 748;
(b) D.O. Shah, J.H. Schulman, J. Lipid Res. 8 (1967) 215.
[42] C.W. McConlogue, T.K. Vanderlick, Langmuir 13 (1997) 7158.
[43] C.W. McConlogue, T.K. Vanderlick, Langmuir 14 (1998) 6556.
[44] C.W. McConlogue, D. Malaud, T.K. Vanderlick, Biochim. Biophys. Acta 1372 (1998) 124.
[45] H.M. Courrier, T.F. Vandamme, M.P. Krafft, S. Nakamura, O. Shibata, Colloids Surf. A 215 (2003) 33.
[46] H. Nakahara, S. Nakamura, S. Lee, G. Sugihara, O. Shibata, Colloids Surf. A 270–271 (2005) 52.